Optimal Power Flow (OPF) Model with Unified AC-DC Load Flow and Optimal Commitment for an AC-catenary Railway Power Supply System (RPSS) fed by a High Voltage DC (HVDC) transmission line

Lars Abrahamsson, *Student Member, IEEE,* Stefan Östlund, *Senior Member, IEEE,* and Lennart Söder, *Member, IEEE*

***Abstract*—In this paper an alternative railway power systems design based on an HVDC feeder is studied. The HVDC feeder is connected to the catenary by converters. Such an HVDC line is also appropriate for DC-fed railways and AC-fed railways working at public frequency.**

A unit commitment optimal power flow model has been developed and is applied on a test system. In this paper, the model is presented in detail. The model, in the form of an MINLP program, uses unified AC-DC power flow to minimize the entire railway power system losses.

Simulations of the proposed solution show clear advantages regarding transmission losses and voltages compared to conventional systems, especially for cases with long distances between feeding points to the catenary, and when there are substantial amounts of regeneration from the trains.

I. Introduction

No model for unified AC-DC power flow combined with unified optimal power flow and optimal commitment of converters have been presented for railway applications before. This was completely new.

THIS paper presents and suggests models for a new way of feeding railway power supply systems (RPSS) that would improve voltage quality and reduce power losses without modifying the catenary line impedances, adding conductors, or adding extra connections between catenary and feeding lines. A feeder concept comprising a multi-terminal HVDC (MTDC) supply line is investigated [1], [2]. Instead of connecting the rectifier and inverter back-to-back as in a conventional static converter station, rectifiers and inverters are interconnected through a distributed DC-bus – the HVDC feeder line. Typically, rectifiers are placed at a fairly large distance, compared to the inverters. Determining the optimum rating and distance of the inverters is outside the scope of this paper. Models for determining the optimal location of RPSS feeders, applied on classical converter stations are presented in [3].

L. Abrahamsson and L. Söder are with the Department of Electrical Power Systems, Royal Institute of Technology (KTH), Stockholm, Sweden, e-mail: (lars.abrahamsson@ee.kth.se & lennart.soder@ee.kth.se).

S Östlund is with with the Department of Electrical Energy Conversion, Royal Institute of Technology (KTH), Stockholm, Sweden, e-mail: (stefan.ostlund@ee.kth.se).

Manuscript received August –, 2012; revised - -, 201-.

This paper presents detailed still-standing-load mathematical models of an optimally-controlled HVDC-fed RPSS and of classically controlled rotary-mimicking-converter fed systems. The latter may also include an HVAC transmission line, which is considered and compared to the HVDC line in one of the examples. The optimality of the HVDC-feeding is with respect to overall system losses and considers the unit commitment of the converters besides the power flow directions and amounts.

The numerical example in Section IV is adapted to Swedish conditions, but the idea in itself is with some generalization applicable to any kind of RPSS – that is; DC, low-frequency AC, and public grid frequency AC catenaries. The mathematical models are if further generalized applicable also without DC-grid, or with the DC-grid exchanged to an AC-grid. AC railway grids with public frequency often just have transformers instead of converter stations, using two of the public grid's three phases. The drawbacks of direct transformer feeding are further treated in [2], [4]–[8].

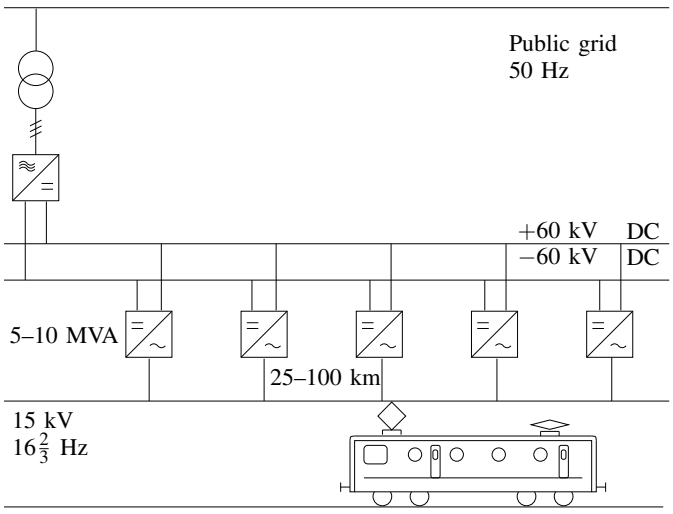

Fig. 1: Visualization of the proposed solution comprising an HVDC feeder line.

II. Background and Contribution

Rail transportation in the world has in recent years risen considerably due to energy-efficiency and climate change, an increase expected to continue. This places greater demands on energy supply both regarding installed power and power/voltage quality. In general, the power demand is critical in areas of dense traffic, such as in metropolitan areas, whereas maintaining the voltage level is the main problem on rural parts of the main lines as well as on some industrial freight lines [2], [9]–[11].

A. AC-DC-load flow

Many AC-DC-load flow methods have been presented, sequential or unified, each method have its pros and cons. For public power systems sequential models have been presented in [12], [13]. An early unified AC-DC power flow method for HVDC-fed public AC grids was presented in [14] where, in order to avoid binary variables, several control modes are defined, of which some allows a decoupled computation model.

A unified AC-DC power flow for DC railways is presented in [15]; whereas a sequential one can be found in [16]. In [17], a literature review of railway AC-DC power flow is presented.

The model presented in this paper is unified, and the methods of solving are handled by standard algorithms. Nonlinear solver choices matters [18].

According to [19] sequential AC-DC power flows are easier to code, whereas simultaneous (unified) are faster to compute. A simplified sequential method is presented in [19] that only needs one iteration for each system, given that taps are within their limits. This paper uses exact methods, and unified power flow.

B. HVDC-fed railways

In [20], HVDC-feeding of an LVDC light-rail system is suggested and presented using moving loads. An optimal control of the converters is presented, minimizing the LVDC catenary losses. The optimal control is compared with "HVDC structure without optimization" which is a bit unclearly defined. In this paper, an HVDC-fed AC catenary is modeled, considering the no-load converter losses, justifying unit commitment. This paper, does not consider moving loads.

C. Benefits with suggested HVDC solution

Using HVDC cables should in most cases be possible without any additional land usage.

The effects of alternating magnetic fields on the human body are unclear. Thus, as a precaution, new overhead lines are usually not permitted in populated areas. Buried cables are also less exposed weather.

D. OPF (Optimal Power Flow)

The term "optimal power flow" was introduced as early as in 1968 [21], and proposed methods for solving the OPF for railways have been found since the 1990's [22]. The term contains a wide range of problems from quite economical studies, through losses minimizations, to conditions on magnetic fields, voltage drops, and such [21].

This paper uses classical optimization modeling and solver software. The alternative to classical models and solvers is using meta-heuristic OPF methods [21].

Many papers focus on the solution methods, whereas this paper focus on the modeling, and use standard algorithms for the optimization and equations solving. The models presented still have to be designed to suit the solvers used.

The OPF problem is thoroughly studied for public grids, for both transmission and distribution. In the railway field, there are less publications available regarding OPF. Therefore much work still remains in finding relevant and efficient models and interesting problem formulations.

An OPF, or generally, power flows, can mainly be expressed in rectangular or polar coordinates, and computationally they are equivalent, c.f. [23]. This paper uses polar coordinates. In [23] a hybrid formulation for NLP OPF is presented. Power mismatch equations are expressed in power for nonzero injection nodes and in current for zero injection nodes, whereas the power flow equations are written in voltage rectangular coordinates. The hybrid model is fast for systems with many zero injection nodes.

1) Public grids: OPF can be studied in many ways, e.g. in [24] the dual of the OPF problem, which can be expressed as a semi-definite problem (SDP) is derived. SDPs can be solved to global optimum in polynomial time, c.f. [24]. It can be verified when the duality gap is zero. The theory of [24] can be applied for many relevant OPF problems. The theory does however not apply for problems containing integer variables, as the problem of this paper does, allowing switching on and off of converters. The model presented in [24] is not applicable for unit commitment problems or other mixed-integer optimizations. Moreover, it is assumed that "active power loss is nonzero, but small, in practice", so it is unclear if the method is applicable on general RPSSs even if leaving the binaries behind. Another SDP model for OPF is presented in [25].

The general OPF is hard to solve [26], so sometimes when solving multi-objective problems, meta-heuristic methods have to be used. In this paper, there is a clear objective, and it is also the authors belief that classical optimization methods are to prefer when possible.

The security constrained OPF is in [27] presented as an NLP using fast decoupled load flow and solved as an SQP (sequential quadratic programming). The solutions are supposed to manage a single outage.

In [28], OPF is done in GAMS for distribution systems. RPSSs are often radial due to the nature of the load they are supplying. There is however no desire to keep the grid un-meshed, actually the desire is the opposite. In distribution systems, the grids are desired to be radial, so the planning is a bit different.

In [28], the problem is solved two-stage, by Benders decomposition. The master problem is MIQCP [29], whereas the slave problem is NLP [29]. The system network configuration involves decision variables opening and closing connections. In this paper, the loss function describes the real losses,

whereas in [28], the losses function is apparent-power dependent.

In [30], parallelizable methods for large-scale distributed OPF are presented. These classify the system into regions, and convexify the problem to make it manageable. Another coordinated decentralized multi-area OPF problem with economic interest and slightly simplified power system description [31], uses "DC-load-flow" with nonlinear terms and a cosine approximation of the losses. Lagrange relaxation decomposition procedures are applied. Normally, RPSS are not region-based in that sense. It happens that mainline RPSSs are connected to metropolitan or suburban power systems, but it is rare.

OPF models can also include and focus on electricity prices and market models. In the mainly education-oriented GUI-based open-source software [32], such OPF is treated. In such studies, the equations describing the power system are not rarely heavily simplified.

In [33] Newton's method is used for public transmission grid voltage/reactive power control, modeled as an NLP where tap changer levels are rounded to possible values after simulation. A suboptimal power flow was determined reducing the set of control variables, supposed to be used by operators. Both losses and the differences of reactive production reserves were minimized.

2) Railway grids: A railway OPF model where the reactive power consumption of trains is controlled is presented in [34]. It is shown that reactive control of modern trains is very beneficial if there are about half modern and half old-fashioned trains in the fleet.

An early railway optimal commitment study [35] treats the converter stations as slack buses, separating the system into power sections, allowing a fast power-flow calculation. The discrepancies from exact power flows can however reach up to 40 %, so a more detailed model like the one presented in this paper can definitely be motivated. In reality, the number of rotary converters committed to a station impacts the power output from neighboring stations.

Railway OPF with a linearized function controlling the active power injections by controlling the voltage phase angles is presented in [22], where one of the converters in the RPSS constitutes a slack bus.

Railway OPF results, minimizing energy costs for DC-fed systems, are presented in [36], the models are however not presented in detail. In [37] a successive LP OPF algorithm, designed for railway usage, is presented. DC railways and the impact of letting various numbers of substations include rectifiers, and/or inverters are studied in [38].

Railway OPF can also consider the difference in electricity prices between different in-feeding public grid operators [39].

III. Modelling

A. Suggested DC Feeder Lines

The feeder line may be implemented as a ground cable. The cable could be a 60 kV dipole with 240 mm^2 aluminium conductors which yields a power handling capability of approximately 50 MW. Such a cable has the impedance

$$R_{line} = 0.1175\ \Omega/\text{km}. \tag{1}$$

B. Converter stations

1) Proposed Converters: The converter losses for inverter mode are modeled as a second order polynomial according to equation (43), where $I_{g_{\mathbf{a}\leftrightarrow d}}$ is the per-unit current on the AC-side of the converter, and $P^{c,i}_{L;g_{\mathbf{a}\leftrightarrow d}}$ is the per-unit power. It is normal that converter losses are modeled as second order polynomials of the AC-side current, c.f. [12], [13]. The quadratic term represents the resistive losses of the converter, whereas the linear term represents constant-voltage-type losses, and the constant term corresponds to idling losses. The polynomial is derived assuming inverter operation at unity power factor, which is when the losses are the highest. This model is used for inverter mode of the converter, regardless of $\cos\phi$. Operating the converter as a rectifier will yield slightly lower losses, in this paper modeled as 0.9 times the inverter losses, c.f. equation (44), also here regardless of $\cos\phi$. The per-unit losses are for simplicity assumed to be independent of the converter ratings. It is however assumed that all the converters used in the case studies are of the same rating, and in Case B the loss functions for each HVDC feeding point are thus doubled.

All harmonics, that can be substantial depending on the type of vehicles, are neglected. The proposed converter solution uses medium frequency transformer technology [2], [40].

2) Classic Converters: If static converters are used, the terminal voltage and phase shift can be controlled freely [4]. However, for easy replacement and inter-operability, static converters are often made to mimic the behavior of rotating converters, i.e. in Sweden, Norway, and parts of Eastern Germany. The characteristics of rotary and rotary-mimicking converters are given in e.g. [41]. The voltage is controlled to be slightly decreasing with increasing reactive load according to equation (68).

In this paper, a lossless model of the converters is used. If the converters would be modeled with losses, $P_{G;g}$ in the first nonlinear term (corresponding to the motor side) of equation (70) should be replaced by a $P_{M;g}$. If $P_{M;g}$ and $P_{G;g}$ would not be the same, some modeling corresponding to equations (41), (43), and (44) would be needed. The motoring power would also have to be introduced in equation (71).

C. Catenary

The catenary is a typical arrangement in Sweden denoted 120 mm^2, 2Å, which means that the cross section of the contact wire is 120 mm^2 with two aluminum BT-system return conductors of each 212 mm^2 cross section area, parallel connected to the track. The impedance

$$Z_{line} = 0.20 + j0.20\ \Omega/\text{km}. \tag{2}$$

This arrangement is relatively weak.

D. Load

In this work, the vehicles are assumed to be equipped with modern voltage source converters (VSC) capable to operate at unity power factor and negligible harmonic currents.

E. Grid Topology

The supplying DC grid is comb-shaped, with a converter station in each comb-pin end. The MTDC grid is connected to the public grid in the upper left part of the down-pointing comb, c.f Figure 1. That is the explanation for that the power inflows are slightly bigger in CE2 than in CE3 in Table VIII. As a consequence, in order to even out the losses between the converters, this is compensated by a slightly greater reactive power production in CE3 than in CE2. CE is in this paper an abbreviation for Connecting Equipment, a generalized RPSS feeder denotation.

The AC-grids – both the one connected to an MTDC feeding grid, and the classical one connected directly to the public grid have the comb pointing upwards. In the proposed solution, the impedances between catenaries and converters results in extra nodes, whereas in the classical cases, these small impedances are included in the converter modeling.

F. Modeling description

The MTDC problem is formulated as an optimization problem where the system active power losses are to be minimized, whereas the studies of the present RPSS is a system of equations to be solved. The mathematical formulations are presented Section III-G.

Parameters, (continuous) variables and binary variables are defined in Tables IV and VI respectively, whereas numerical values of most parameters are presented in Table V.

1) The HVDC-fed OPF system: The objective function, the total losses, $\min P_L$, to be minimized is stated in equation (67). Minimization is done subject to the bounds of equations (5)–(24) and to the constraints of equations (33)–(67). The initial variable levels are not presented in this paper dues to less importance and space limitations.

The converters are modeled as twin-nodes (one AC-node and one DC-node strongly related to each other), c.f. equation (41), where the (active) power consumed on one side equals the (active) power injected on the other side, plus the converter losses. That is a special kind of power mismatch equation. The converter losses for inverting mode are described by equation (43), whereas the losses when rectifying are described by equation (44). Converter losses are bounded below by $P_{L,\max}$ if turned on, and by 0 if turned off, c.f. equation (51). Converter losses equal the inverting losses if turned on and inverting, c.f. equations (52) and (53). Converter losses equal the rectifying losses if turned on and not inverting, c.f. equations (54) and (55).

Converter apparent power is defined by equation (46), whereas the converter currents are defined by equation (42).

Apparent power is limited on the AC side, (45) where a voltage level drop at the converter terminal, forces the maximum converted power to drop accordingly, and equation (62) forces the converter apparent power down to zero if switched off; reactive power is limited on the AC side, by voltage level in (49) and (50) and by unit commitment in (60), and (61); and active power is limited on the DC side by currents in (47), (48), and in sign by (63) and (64), and by commitment in (65), and (66); and on the AC side directionwise by (56) and (57), and by commitment in equations (58) and (59). Some of these limits are inspired by and concretized from the ones presented in [7], [12]. Details like converter filters, and/or inside-converter transformers are not considered. The DC system is fed by an infinitely strong lossless three-phase-AC-to-DC converter.

Finally, (33), (34), and (35) are power flow equations; (36), (37), and (38) are the power mismatch equations; and (39) and (40) are conductor losses equations.

2) The classically controlled system: When solving the classical problem, the system of equations (34), (35), (37), (38), (68) – voltage control of RPSS side of converter, (69), (70) – voltage phase angle shifts caused by motor and generator, and (71) – modeling the public grid phase shift due to railway loading is solved. The losses are calculated manually after solving that system of equations. In the classical feeding solution, converter losses are not studied, but models that could be implemented are present in e.g. [41].

G. Mathematical Modelling

The set definitions for the classical converter control, are presented in Table III. For the MTDC studies, they are presented in two different tables. For Case A, Table I, and for for Case B Table II. Unitless electrical parameters and variables are, if presented as dimensionless, expressed in per-unit (p.u.).

TABLE I: Sets, Case A, MTDC problem

Set	Description
$a, a_2 \in \{1,2,...,8,17\}$	AC nodes index
$d, d_2 \in \{9,10,...,16\}$	DC nodes index
$g_{p\leftrightarrow d}(d) \in \{13\}$	Public grid to MTDC grid converter
$g_{\mathbf{a}\leftrightarrow d}(a) \in \{5,6,7,8\}$	The HVDC-AC converter nodes, AC side
$g_{a\leftrightarrow \mathbf{d}}(d) \in \{9,10,11,12\}$	The HVDC-AC converter nodes, DC side
$a_\theta(a) \in \{5\}$	The reference angle node, AC side
$n_{l,d}(d) \in \{13,14,15,16\}$	The DC nodes with no loads
$n_{g,d}(d) \in \{9,10,11,12,14,15,16\}$	The DC nodes with no generation
$n_{g,a}(a) \in \{1,2,3,4,17\}$	The AC nodes with no generation

TABLE II: Sets, Case B, MTDC problem

Set	Description
$a, a_2 \in \{1,2,3,4,9,10\}$	AC nodes index
$d, d_2 \in \{5,6,7,8\}$	DC nodes index
$g_{p\leftrightarrow d}(d) \in \{7\}$	Public grid to MTDC grid converter
$g_{\mathbf{a}\leftrightarrow d}(a) \in \{3,4\}$	The HVDC-AC converter nodes, AC side
$g_{a\leftrightarrow \mathbf{d}}(d) \in \{5,6\}$	The HVDC-AC converter nodes, DC side
$a_\theta(a) \in \{3\}$	The reference angle node, AC side
$n_{l,d}(d) \in \{7,8\}$	The DC nodes with no loads
$n_{g,d}(d) \in \{5,6,8\}$	The DC nodes with no generation
$n_{g,a}(a) \in \{1,2,9,10\}$	The AC nodes with no generation

Parameters are defined numerically in Table V where $I_{\max}$ is the maximal converter current of each converter in a station, calculated such that the converter should be able to deliver rated power at voltage levels of at least 0.8 p.u., and where

TABLE III: Sets, All cases, Classical converter control.

Set	Description
$a, a_2 \in \{1,2,...,9\}$	AC nodes index, Case A
$a, a_2 \in \{1,2,3,4\}$	AC nodes index, Case B
$g, g_2\,(a) \in \{1,9\}$	The rotating converter nodes, Case A
$g, g_2\,(a) \in \{1,4\}$	The rotating converter nodes, Case B
$g_n\,(a) \in \{2,3,...,8\}$	The non-rotating-converter nodes, Case A
$g_n\,(a) \in \{2,3\}$	The non-rotating-converter nodes, Case B
$t\,(a) \in \{5\}$	Nodes with trains, Case A
$t\,(a) \in \{2,3\}$	Nodes with trains, Case B

TABLE IV: Parameters

Parameter	Description
G^a_{a,a_2}	Real part of AC-side admittance matrix (conductance)
B^a_{a,a_2}	Imaginary part of AC-side admittance matrix (susceptance)
G^d_{d,d_2}	DC-side conductance matrix
$P^a_{D;a}$	Active power loads on AC-side, i.e. trains
$Q^a_{D;a}$	Reactive power loads on AC-side, i.e. trains
$U_{G;g_{p\leftrightarrow d}}$	Fixed voltage level on DC-side of public grid to MTDC grid converter
$C_{g_{\mathbf{a}\leftrightarrow d},g_{a\leftrightarrow\mathbf{d}}}$	Binary matrix connecting DC-sides and AC-sides of converter stations
S_b	Base power
$\#^{\text{conv}}$	Number of converters per station
$I_{\max}$	Maximal converter current per converter (unit)
$P_{L,\max}$	Upper bound on converter station losses
$S_{\max}$	Upper bound on converter station apparent power
$P_{\max}$	Upper bound on converter station active power
$Q_{\max}$	Upper bound on converter station reactive power
U^0_g	The terminal no-load voltage level on catenary side of classical converter
k_q	Constant for classical converter voltage control
$\theta^{50;g}$	The no-load angle of the public grid
x_{qM}	Motor-side inner reactance of rotary converter Q48/Q49
x_{qG}	Generator-side inner reactance of rotary converter Q48/Q49
X^{50}_g	The short-circuit reactance of the public grid
$Q_{50;g}$	Reactive power consumption on the motoring side
$U_{M;g}$	Motor-side voltage level

$P_{L,\max}$ is calculated according to equation (43). Since the loss function is defined for one converter, in a station with many converters, the losses has to be multiplied with the number of converters. Train loads are given from the case descriptions, conductances and susceptances are given from equations (1) and (2), and from the case descriptions. The matrix $C_{g_{\mathbf{a}\leftrightarrow d},g_{a\leftrightarrow\mathbf{d}}}$ is constructed such that it is only one for the right combination of converter nodes, e.g. for Case A that would be

$$C_{5,9} = C_{6,10} = C_{7,11} = C_{8,12} = 1 \tag{3}$$

and

$$C_{g_{\mathbf{a}\leftrightarrow d},g_{a\leftrightarrow\mathbf{d}}} = 0 \tag{4}$$

TABLE V: Given numerical values of parameters

Parameter and numerical value					
S_b	5 MVA	$S_{\max}$	$\#^{\text{conv}}$	$P_{\max}$	$\#^{\text{conv}}$
$I_{\max}$	$\frac{1}{0.8}$	$U_{G;g_{p\leftrightarrow d}}$	1	U^0_g	1.1
$Q_{\max}$	$\#^{\text{conv}}$	k_q	20 MVAr/kV	x_{qM}	49 %
x_{qG}	53 %	X^{50}_g	15 %	$Q_{50;g}$	0
$U_{M;g}$	1	$P_{L,\max}$	$\#^{\text{conv}}\left(0.0135I^2_{\max}+0.0097I_{\max}+0.015\right)$		

for all other combinations of $g_{\mathbf{a}\leftrightarrow d}, g_{a\leftrightarrow\mathbf{d}}$. This is used in equation (41) to ensure that power flowing out of the DC grid comes in at the right point in the AC grid, and vice versa. The constant k_q of Table V is defined under the assumption that U and U_0 are given in kV and Q_G is given in MVAr in (68).

TABLE VI: Variables

Variable	Description
U^a_a	Voltage level in AC node
U^d_d	Voltage level in DC node
θ_a	Voltage angle in AC node
P^a_a	Net injected active power at AC bus
P^d_d	Net injected power at DC bus
Q^a_a	Net injected reactive power at AC bus
$P^d_{D;d}$	Power loads on DC-side, i.e. converter stations connecting DC grid to catenary.
$P^a_{G;a}$	Active power generation on AC-side, i.e. converter stations connecting DC grid to catenary.
$Q^a_{G;a}$	Reactive power generation on AC-side, i.e. converter stations connecting DC grid to catenary.
$P^d_{G;d}$	Power generation on DC-side, i.e. converter stations connecting DC grid to public grid.
P_L	Total losses in the entire railway power supply system
$P^a_{L;a}$	Marginal losses for each node in the AC grid conductors
$P^d_{L;d}$	Marginal losses for each node in the DC grid conductors
$P^c_{L;g_{\mathbf{a}\leftrightarrow d}}$	Losses in the converters connecting DC grid to catenaries
$P^{c,i}_{L;g_{\mathbf{a}\leftrightarrow d}}$	Losses in the converters connecting DC grid to catenaries, due to inverting
$P^{c,r}_{L;g_{\mathbf{a}\leftrightarrow d}}$	Losses in the converters connecting DC grid to catenaries, due to rectifying
$I_{g_{\mathbf{a}\leftrightarrow d}}$	The AC-side currents of the converters connecting the DC grid the catenaries.
$S_{g_{\mathbf{a}\leftrightarrow d}}$	The AC-side apparent power of the converters connecting the DC grid the catenaries.
$\Psi_{0;g}$	The phase angle of the public grid in the classical model
$\Psi_{G;g}$	The phase angle shift due to generator of converter in the classical model
$\Psi_{M;g}$	The phase angle shift due to motor of converter in the classical model
$\alpha_{g_{\mathbf{a}\leftrightarrow d}}$	Tell whether the converter station connecting MTDC grid to catenary is inverting (1) or rectifying (0), **binary**
$\gamma_{g_{\mathbf{a}\leftrightarrow d}}$	Tells whether the converter station is committed (1) or not (0), **binary**

These variables' upper, and lower bounds are listed in equations (5)–(32). Typically, good cold-start level values should be in the middle of the range of possible or probable values of a variable [23]. In this paper, some level values are in the middle, and some close to the expected result.

$$0 \le P_L \le 5 \tag{5}$$
$$-P_{\max} \le P^a_{G;g_{\mathbf{a}\leftrightarrow d}} \le P_{\max} \tag{6}$$
$$0 \le P^a_{G;n_{g,a}} \le 0 \tag{7}$$
$$-5 \le P^d_{G;g_{p\leftrightarrow d}} \le 5 \tag{8}$$
$$0 \le P^d_{G;n_{g,d}} \le 0 \tag{9}$$
$$-P_{\max} \le P^d_{D;g_{a\leftrightarrow\mathbf{d}}} \le P_{\max} \tag{10}$$
$$0 \le P^d_{D;n_{l,d}} \le 0 \tag{11}$$
$$-Q_{\max} \le Q^a_{G;g_{\mathbf{a}\leftrightarrow d}} \le Q_{\max} \tag{12}$$
$$0 \le Q^a_{G;n_{g,a}} \le 0 \tag{13}$$
$$0 \le S_{g_{\mathbf{a}\leftrightarrow d}} \le S_{\max} \tag{14}$$
$$-\pi \le \theta_a \le \pi \tag{15}$$

$$0 \leq \theta_{a_\theta} \leq 0 \tag{16}$$
$$0.4 \leq U^a_{n_{g,a}} \leq 1.3 \tag{17}$$
$$0.4 \leq U^a_{g_{\mathbf{a}\leftrightarrow d}} \leq 1.1 \tag{18}$$
$$0.95 \leq U^d_{n_{g,d}} \leq 1.05 \tag{19}$$
$$1 \leq U^d_{g_{p\leftrightarrow d}} \leq 1 \tag{20}$$
$$0.0 \leq I_{g_{\mathbf{a}\leftrightarrow d}} \leq I_{\max} \tag{21}$$
$$0.0 \leq P^c_{L;g_{\mathbf{a}\leftrightarrow d}} \leq P_{L,\max} \tag{22}$$
$$0.0 \leq P^{c,i}_{L;g_{\mathbf{a}\leftrightarrow d}} \leq P_{L,\max} \tag{23}$$
$$0.0 \leq P^{c,r}_{L;g_{\mathbf{a}\leftrightarrow d}} \leq 0.9 \cdot P_{L,\max} \tag{24}$$
$$0.4 \leq U^a_a \leq 1.2 \tag{25}$$
$$-\frac{\pi}{2} \leq \theta^a_a \leq \frac{\pi}{18} \tag{26}$$
$$-2 \leq P^a_{G;g} \leq 2 \tag{27}$$
$$0 \leq P^a_{G;g_n} \leq 0 \tag{28}$$
$$-2 \leq Q^a_{G;g} \leq 2 \tag{29}$$
$$0 \leq Q^a_{G;g_n} \leq 0 \tag{30}$$
$$-\frac{\pi}{2} \leq \Psi_{0;g} \leq \frac{\pi}{9} \tag{31}$$
$$-\frac{11\pi}{18} \leq \Psi_{G;g} + \Psi_{M;g} \leq \frac{\pi}{9} \tag{32}$$

where, the constraints to be used in optimization, or the equations to be used in equation solving, are in (33)–(71).

$$P^d_d = U^d_d \sum_{d_2} U^d_{d_2} G^d_{d,d_2} \tag{33}$$
$$P^a_a = U^a_a \sum_{a_2} \left(U^a_{a_2} G^a_{a,a_2} \cos\left(\theta_a - \theta_{a_2}\right) + + B^a_{a,a_2} \sin\left(\theta_a - \theta_{a_2}\right) \right) \tag{34}$$
$$Q^a_a = U^a_a \sum_{a_2} \left(U^a_{a_2} G^a_{a,a_2} \sin\left(\theta_a - \theta_{a_2}\right) - - B^a_{a,a_2} \cos\left(\theta_a - \theta_{a_2}\right) \right) \tag{35}$$
$$P^d_d = P^d_{G;d} - P^d_{D;d} \tag{36}$$
$$P^a_a = P^a_{G;a} - P^a_{D;a} \tag{37}$$
$$Q^a_a = Q^d_{G;a} - Q^a_{D;a} \tag{38}$$
$$P^a_{L;a} = U^a_a \sum_{a_2} G^a a, a_2 \left(U^a_{a_2} \cos\left(\theta_a - \theta_{a_2}\right) - U^a_a \right) \tag{39}$$
$$P^d_{L;d} = U^d_d \sum_{d_2} G^d d, d_2 \left(U^d_{d_2} - U^d_d \right) \tag{40}$$
$$0 = \sum_{g_{a\leftrightarrow \mathbf{d}}} \left(P^a_{G;g_{\mathbf{a}\leftrightarrow d}} - P^d_{D;g_{a\leftrightarrow \mathbf{d}}} + + P^c_{L;g_{\mathbf{a}\leftrightarrow d}} \right) C_{g_{\mathbf{a}\leftrightarrow d}, g_{a\leftrightarrow \mathbf{d}}} \tag{41}$$
$$S^a_{G;g_{\mathbf{a}\leftrightarrow d}} = I_{g_{\mathbf{a}\leftrightarrow d}} \cdot \#^{\text{conv}} \cdot U^a_{g_{\mathbf{a}\leftrightarrow d}} \tag{42}$$
$$P^{c,i}_{L;g_{\mathbf{a}\leftrightarrow d}} = \#^{\text{conv}} \cdot \left(0.0135 \left(I_{g_{\mathbf{a}\leftrightarrow d}} \right)^2 + 0.0097 I_{g_{\mathbf{a}\leftrightarrow d}} + + 0.015 \right) \tag{43}$$
$$P^{c,r}_{L;g_{\mathbf{a}\leftrightarrow d}} = \#^{\text{conv}} \cdot \left(0.0135 \left(I_{g_{\mathbf{a}\leftrightarrow d}} \right)^2 + 0.0097 I_{g_{\mathbf{a}\leftrightarrow d}} + + 0.015 \right) \cdot 0.9 \tag{44}$$
$$S_{g_{\mathbf{a}\leftrightarrow d}} \leq U^a_{g_{\mathbf{a}\leftrightarrow d}} \cdot I_{\max} \cdot \#^{\text{conv}} \tag{45}$$
$$0 = \left(P^a_{G;g_{\mathbf{a}\leftrightarrow d}} \right)^2 + \left(Q^a_{G;g_{\mathbf{a}\leftrightarrow d}} \right)^2 - \left(S_{g_{\mathbf{a}\leftrightarrow d}} \right)^2 \tag{46}$$
$$P^d_{D;g_{a\leftrightarrow \mathbf{d}}} \leq U^d_{g_{a\leftrightarrow \mathbf{d}}} \cdot I_{\max} \cdot \#^{\text{conv}} \tag{47}$$
$$P^d_{D;g_{a\leftrightarrow \mathbf{d}}} \geq -U^d_{g_{a\leftrightarrow \mathbf{d}}} \cdot I_{\max} \cdot \#^{\text{conv}} \tag{48}$$
$$Q^a_{G;g_{\mathbf{a}\leftrightarrow d}} \leq U^a_{g_{\mathbf{a}\leftrightarrow d}} \cdot I_{\max} \cdot \#^{\text{conv}} \tag{49}$$
$$Q^a_{G;g_{\mathbf{a}\leftrightarrow d}} \geq -U^a_{g_{\mathbf{a}\leftrightarrow d}} \cdot I_{\max} \cdot \#^{\text{conv}} \tag{50}$$
$$P^c_{L;g_{\mathbf{a}\leftrightarrow d}} \leq P_{L,\max} \cdot \gamma_{g_{\mathbf{a}\leftrightarrow d}} \tag{51}$$
$$P^c_{L;g_{\mathbf{a}\leftrightarrow d}} \geq P^{c,i}_{L;g_{\mathbf{a}\leftrightarrow d}} - P_{L,\max} \left(2 - \alpha_{g_{\mathbf{a}\leftrightarrow d}} - \gamma_{g_{\mathbf{a}\leftrightarrow d}} \right) \tag{52}$$
$$P^c_{L;g_{\mathbf{a}\leftrightarrow d}} \leq P^{c,i}_{L;g_{\mathbf{a}\leftrightarrow d}} + P_{L,\max} \left(2 - \alpha_{g_{\mathbf{a}\leftrightarrow d}} - \gamma_{g_{\mathbf{a}\leftrightarrow d}} \right) \tag{53}$$
$$P^c_{L;g_{\mathbf{a}\leftrightarrow d}} \geq P^{c,r}_{L;g_{\mathbf{a}\leftrightarrow d}} - P_{L,\max} \left(1 + \alpha_{g_{\mathbf{a}\leftrightarrow d}} - \gamma_{g_{\mathbf{a}\leftrightarrow d}} \right) \tag{54}$$
$$P^c_{L;g_{\mathbf{a}\leftrightarrow d}} \leq P^{c,r}_{L;g_{\mathbf{a}\leftrightarrow d}} + P_{L,\max} \left(1 + \alpha_{g_{\mathbf{a}\leftrightarrow d}} - \gamma_{g_{\mathbf{a}\leftrightarrow d}} \right) \tag{55}$$
$$P^a_{G;g_{\mathbf{a}\leftrightarrow d}} \leq P_{\max} \cdot \alpha_{g_{\mathbf{a}\leftrightarrow d}} \tag{56}$$
$$P^a_{G;g_{\mathbf{a}\leftrightarrow d}} \geq -P_{\max} \left(1 - \alpha_{g_{\mathbf{a}\leftrightarrow d}} \right) \tag{57}$$
$$P^a_{G;g_{\mathbf{a}\leftrightarrow d}} \leq P_{\max} \cdot \gamma_{g_{\mathbf{a}\leftrightarrow d}} \tag{58}$$
$$P^a_{G;g_{\mathbf{a}\leftrightarrow d}} \geq -P_{\max} \cdot \gamma_{g_{\mathbf{a}\leftrightarrow d}} \tag{59}$$
$$Q^a_{G;g_{\mathbf{a}\leftrightarrow d}} \leq Q_{\max} \cdot \gamma_{g_{\mathbf{a}\leftrightarrow d}} \tag{60}$$
$$Q^a_{G;g_{\mathbf{a}\leftrightarrow d}} \geq -Q_{\max} \cdot \gamma_{g_{\mathbf{a}\leftrightarrow d}} \tag{61}$$
$$S^a_{G;g_{\mathbf{a}\leftrightarrow d}} \leq S_{\max} \cdot \gamma_{g_{\mathbf{a}\leftrightarrow d}} \tag{62}$$
$$P^d_{D;g_{a\leftrightarrow \mathbf{d}}} \leq P_{\max} \sum_{g_{\mathbf{a}\leftrightarrow d}} \alpha_{g_{\mathbf{a}\leftrightarrow d}} C_{g_{\mathbf{a}\leftrightarrow d}, g_{a\leftrightarrow \mathbf{d}}} \tag{63}$$
$$P^d_{D;g_{a\leftrightarrow \mathbf{d}}} \geq -P_{\max} \sum_{g_{\mathbf{a}\leftrightarrow d}} \left(1 - \alpha_{g_{\mathbf{a}\leftrightarrow d}} \right) C_{g_{\mathbf{a}\leftrightarrow d}, g_{a\leftrightarrow \mathbf{d}}} \tag{64}$$
$$P^d_{D;g_{a\leftrightarrow \mathbf{d}}} \leq P_{\max} \sum_{g_{\mathbf{a}\leftrightarrow d}} \gamma_{g_{\mathbf{a}\leftrightarrow d}} C_{g_{\mathbf{a}\leftrightarrow d}, g_{a\leftrightarrow \mathbf{d}}} \tag{65}$$
$$P^d_{D;g_{a\leftrightarrow \mathbf{d}}} \geq -P_{\max} \sum_{g_{\mathbf{a}\leftrightarrow d}} \gamma_{g_{\mathbf{a}\leftrightarrow d}} C_{g_{\mathbf{a}\leftrightarrow d}, g_{a\leftrightarrow \mathbf{d}}} \tag{66}$$
$$P_L = \sum_a P^a_{L;a} + \sum_d P^d_{L;d} + \sum_{g_{\mathbf{a}\leftrightarrow d}} P^c_{L;g_{\mathbf{a}\leftrightarrow d}} \tag{67}$$
$$U_g = U^0_g - \frac{Q_{G;g}}{k_q \#^{\text{conv}}} \tag{68}$$
$$\theta_g = \Psi_{0;g} + \Psi_{M;g} + \Psi_{G;g} \tag{69}$$
$$0 = \Psi_{M;g} + \Psi_{G;g} + + \frac{1}{3} \arctan\left(\frac{x_{qM} \cdot \frac{P_{G;g}}{\#^{\text{conv}}}}{U^2_{M;g} + x_{qM} \cdot \frac{Q_{50;g}}{\#^{\text{conv}}}} \right) + + \arctan\left(\frac{x_{qG} \cdot \frac{P_{G;g}}{\#^{\text{conv}}}}{U^2_{G;g} + x_{qG} \cdot \frac{Q_{G;g}}{\#^{\text{conv}}}} \right), \tag{70}$$
$$\Psi_{0;g} = \theta^{50}_g - \frac{1}{3} \arctan\left(\frac{X^{50}_g P_{G;g}}{U^2_{M;g} + X^{50} Q_{50;g}} \right) \tag{71}$$

IV. Comparative Case Studies

A comparison has been made between existing solutions and the suggested one. Two different test cases have been simulated and compared. The test cases were chosen to illustrate important properties of the system, like commitment of converters and the ability for regeneration.

The numerical examples are inspired by the 15 kV $16\frac{2}{3}$ Hz RPSS of Sweden. A comparison is made how the system acts now and how it acts when replacing present converters and transformer substations with HVDC feeding and controlling it optimally rather than following the classical control schemes. For details of how the Swedish RPSS is constituted, please refer to [42]–[44].

The modeling software GAMS [29] have been used. For the cases where systems of equations were about to be solved, a CNS problem class was defined, solved using the CONOPT [45] algorithm. For the OPF cases the problem was modeled as an MINLP problem using the local solver algorithm BONMIN [45]. Global solvers like COUENNE [45] have been tried for small test cases when the respective solutions corresponded very well. Due to extensive computational times, global solving can not be done for all the studied cases.

In the OPF problems, voltage level and angle on the converters were controllable with regard to installed apparent power, and other physical limitations. The converters could be either online or offline, and rectifying or inverting; giving rise to different loss functions. This all was subject to minimization of the total power losses in the system.

TABLE VII: Summary of results

	Case A CCC	Case A OPF	Case B CCC	Case B OPF
Base voltage		15 kV		
Base power		5 MVA		
Min. voltage	1.051	1.057	0.982	1.012
Max. voltage	1.099	1.100	1.147	1.162
Conversion losses	–	0.060	–	0.087
Transmission losses AC	0.071	0.064	0.454	0.223
Transmission losses DC	–	0.004	–	0.006
Total losses	–	0.128	–	0.316

TABLE VIII: Excerpt of results, Case A.

	CE1	CE2	CE3	CE4
$P^d_{D;g_{a\leftrightarrow \mathbf{d}}(d)}$	0.000	0.866	0.858	0.000
$P^d_{G;g_{\mathbf{a}\leftrightarrow d}(a)}$	0.000	0.836	0.828	0.000
$Q^d_{G;g_{\mathbf{a}\leftrightarrow d}(a)}$	0.000	0.029	0.036	0.000
$P_{G;1}, P^a_{3,4}, P^a_{7,6}, P_{G;9}$	0.835	−0.709	−0.709	0.835
$Q_{G;1}, Q^a_{3,4}, Q^a_{7,6}, Q_{G;9}$	0.048	−0.107	−0.107	0.048
$P^a_{1,2}, -, -, P^a_{9,8}$	0.711	-	-	0.711
$P^a_{1,3}, -, -, P^a_{9,7}$	0.125	-	-	0.125
OPF voltages				
$U^a_1, U^a_2, U^a_3, U^a_4$	1.100	1.100	1.100	1.100
$U^a_5, U^a_6 U^a_7 U^a_8$	1.100	1.100	1.100	1.100
CCC voltages				
$U^a_1, U^a_3, U^a_7, U^a_9$	1.099	1.094	1.094	1.099
Train Load	OPF: $P^a_{D;17} = 1.600$		CCC: $P^a_{D;5} = 1.600$	
Train Voltage	OPF: $U^a_{17} = 1.057$		CCC: $U^a_5 = 1.051$	

a) Case A: Single motoring train and 25 km between CEs: This case was chosen in order to be able to compare two kinds of centralized RPSS. The classical with transformers connecting the transmission line and the catenary between the converters, and the proposed one where both converters and transformers are replaced by HVDC converter stations. The train is located in the middle of the section. The power consumed by the train is 8 MW at unity power factor. The two centrally located transformers are rated to 16 MVA , whereas the leftmost and rightmost transformers are rated to 25 MVA. The classical converters are connected to the catenary.

The solutions for both OPF and classical control are displayed in Table VIII. The voltage at the pantograph is above 15.7 kV which means that the performance of the locomotive is unaffected [46]. The losses are dominated by transmission losses but both transmission losses and conversion losses are of the same magnitude.

The transmission losses are slightly bigger in the classical feeding solution, whereas the pantograph voltage levels typically are the same, c.f. Tables VII and VIII.

TABLE IX: Excerpt of results, Case B.

	CE1	CE2	CE1	CE2
$P^d_{D;g_{a\leftrightarrow \mathbf{d}}(d)}$, $P^d_{G;g_{\mathbf{a}\leftrightarrow d}(a)}$	−0.900	1.210	−0.939	1.162
$Q^d_{G;g_{\mathbf{a}\leftrightarrow d}(a)}$	0.077	0.145	-	-
$P_{G;1}, P_{G;4}, Q_{G;1}, Q_{G;9}$	−0.346	0.800	−0.272	0.726
OPF				
$U^a_1, U^a_2, U^a_3, U^a_4$	1.100	1.099	1.100	1.100
Train Load	$P^a_{D;9} = -1.600$		$P^a_{D;10} = 1.600$	
Train Voltage	$U^a_9 = 1.162$		$U^a_{10} = 1.012$	
CCC				
$U^a_1, U^a_4, -, -$	1.105	1.088	-	-
Train Load	$P^a_{D;2} = -1.600$		$P^a_{D;3} = 1.600$	
Train Voltage	$U^a_2 = 1.147$		$U^a_3 = 0.982$	

b) Case B: One motoring train and one braking train and 100 km between CEs: This case illustrates power flow during regenerative braking on a typical line with CEs located 100 km from each other. Normally, feedback to the national grid is not appreciated by public grid owners. Therefore, in the MTDC case the impact is studied when it is not allowed to feed back to the public grid from the MTDC grid.

The distance between the trains is 66.7 km and the distance to the closest converter station is 16.7 km, for both of the trains. The active and reactive power consumptions of the two locomotives are the same and equal to Case A, with the exception that one of them regenerates, and the other one is motoring.

About 60 % of the power is regenerated to the HVDC line and fed back to the consuming train. The remaining regenerated power is transmitted through the catenary line. The AC losses are almost halved in the OPF case compared to the classical one, c.f. Table VII. In the OPF case, the converter losses are less than half of the transmission losses. The minimum voltage levels are above 15 kV for OPF study, and not far from it in the classical feeding study.

V. Conclusions & Discussion

There is a significant difference in the power flow results between the simulated system with converter control according to Swedish regulations and the HVDC OPF solution. The difference is most pronounced in the case with regenerative braking and comparatively long inter-converter distance, Case B, where the classical AC transmission losses are more than twice the OPF losses. The difference is caused by a significant power flow through the catenary when no controllable HVDC-feeder is present. With HVDC-supplied railways, the inter-converter distances can be far without causing unbearable losses. As can be seen comparing cases A and B, the centralized solution is better than without any transmission lines at all [22]. One key issue for the optimal solution is the exact

modeling of the converter losses. The proposed system handles regenerative braking well even over large distances.

In real-life, it is not possible to exactly know all momentary load levels, load positions and levels of power conversion. Therefore, a truly optimal solution is not achievable in a future application. The benefit of determining the optimal solution is however that it sets a theoretical upper bound on how small the losses possibly can be using a smart control strategy. That is, the minimum losses shows the potential of the technology – but not how to implement the solution.

A quest for future studies is to examine control rules based upon traffic in the power system sections connected to the converter being controlled, and power system measurements from adjacent converters. Robust approaches could be stochastic optimization models, e.g. chance constrained OPF [47] but applied to the railway, but also simpler variants such as creating a control law for converters by studying various OPF solutions.

REFERENCES

[1] T. Lejonberg, "Plant for feeding alternating voltage," May 1998. Patent. URL: http://www.wipo.int/patentscope/search/en/WO1998055339.

[2] L. Abrahamsson, T. Kjellqvist, and S. Östlund, "HVDC Feeder Solution for Electric Railways," *IET Power Electronics*, 2012. Accepted for publication.

[3] L. Abrahamsson and L. Söder, "Railway power supply investment decisions considering the voltage drops - assuming the future traffic to be known," in *Intelligent System Applications to Power Systems, 2009. ISAP '09. 15th International Conference on*, pp. 1–6, 2009.

[4] L. Abrahamsson, T. Schütte, and S. Östlund, "Use of converters for feeding of ac railways for all frequencies," *Elsevier Energy for Sustainable Development*, 2012. Accepted for publication.

[5] U. Behmann and T. Schütte, "Static converters – the future of traction power supply," *Rail Technology Review*, vol. 1, pp. 9–15, 2012.

[6] U. Behmann and K. Rieckhoff, "Converter Stations in 50 or 60 Hz Traction Power Supply," *Rail Technology Review*, vol. 51, no. 4, pp. 8 – 14, 2011.

[7] U. Behmann and K. Rieckhoff, "Umrichterwerke bei 50 Hz-Bahnen - Vorteile am Beispiel der Chinese Railways/Converter Stations in 50 Hz Traction - Advantages in Case of Chinese Railways.," *Elektrische Bahnen*, vol. 109, no. 1–2, pp. 63–74, 2011.

[8] T. Schütte and U. Behmann, "Converters in the railway power supply – worldwide chances (original title in german)," *Elektrische Bahnen*, vol. 109, no. 4–5, pp. 254–257, 2011.

[9] L. Abrahamsson and L. Söder, "Fast Estimation of Relations between Aggregated Train Power System Data and Traffic Performance," *IEEE Journal of Vehicular Technology*, vol. 60, pp. 16–29, Jan. 2011.

[10] C. J. Goodman, "Overview of electric railway systems and the calculation of train performance," *Electric Traction Systems, 2008 IET Proffessional Development course on*, pp. 1–24, Nov. 2008.

[11] R. J. Hill, "Electric railway traction, Part 3 Traction power supplies," *Power Engineering Journal*, vol. 8, pp. 275–286, Dec. 1994.

[12] J. Beertens, S. Cole, and R. Belmans, "Generalized steady-state vsc mtdc model for sequential ac/dc power flow algorithms," *Power Systems, IEEE Transactions on*, vol. PP, pp. 1–9, Jan. 2012.

[13] J. Beertens, S. Cole, and R. Belmans, "A sequential AC/DC power flow algorithm for networks containing Multi-terminal VSC HVDC systems," in *Power and Energy Society General Meeting, 2010 IEEE*, 2010.

[14] T. Smed, G. Andersson, G. Sheble, and L. Grigsby, "A new approach to ac/dc power flow," *Power Systems, IEEE Transactions on*, vol. 6, pp. 1238 – 1244, Aug. 1991.

[15] Y.-S. Tzeng, R.-N. Wu, and N. Chen, "Unified ac/dc power flow for system simulation in dc electrified transit railways," *Electric Power Applications, IEE Proceedings*, vol. 142, pp. 345–354, Nov. 1995.

[16] C. L. Pires, S. I. Nabeta, and J. R. Cardoso, "Dc traction load flow including ac distribution network," *IET Electric Power Applications*, vol. 3, pp. 289–297, 2009.

[17] P. Arboleya, G. Diaz, and M. Coto, "Unified ac/dc power flow for traction systems: A new concept," *IEEE Journal of Vehicular Technology*, 2012. Accepted for publication.

[18] T. Lastusilta, M. R. Bussieck, and T. Westerlund, "Comparison of some high-performance minlp solvers," *Chemical Engineering Transactions*, vol. 11, pp. 125–130, 2007.

[19] H. Fudeh, "A simple and efficient ac-dc load-flow method for multiterminal dc systems," *Power Apparatus and Systems, IEEE Transactions on*, vol. PAS-100, pp. 4389 – 4396, Nov. 1981.

[20] R. Vial, D. Riu, and N. Retière, "Simulating calculations and optimization design of a new hvdc supply power for light rail system," in *IECON 2010 - 36th Annual Conference on IEEE Industrial Electronics Society*, (Nov.), pp. 2364 – 2369, 2010.

[21] M. AlRashidi and M. El-Hawary, "Applications of computational intelligence techniques for solving the revived optimal power flow problem," *Electric Power Systems Research*, vol. 79, pp. 694–702, Apr. 2009.

[22] M. Olofsson, G. Andersson, and L. Söder, "Optimal operation of the swedish railway electrical system," in *Electric Railways in a United Europe, 1995., International Conference on*, pp. 64–68, Mar. 1995.

[23] Q. Jiang, H.-D. Chiang, C. Guo, and Y. Cao, "Power-current hybrid rectangular formulation for interior-point optimal power flow," *Generation, Transmission & Distribution, IET*, vol. 3, pp. 748–756, Aug. 2009.

[24] J. Lavaei, "Zero duality gap in optimal power flow problem," *Power Systems, IEEE Transactions on*, vol. 27, pp. 92 – 107, Feb. 2012.

[25] X. Bai, H. Weia, K. Fujisawa, and Y. Wang, "Semidefinite programming for optimal power flow problems," *International Journal of Electrical Power & Energy Systems*, vol. 30, pp. 383–392, July- 2008.

[26] T. Niknam, M. rasoul Narimani, M. Jabbari, and A. R. Malekpour, "A modified shuffle frog leaping algorithm for multi-objective optimal power flow," *Energy*, vol. 36, p. 64206432, Nov. 2011.

[27] H. Harsan, N. Hadjsaid, and P. Pruvot, "Cyclic security analysis for security constrained optimal power flow," *Power Systems, IEEE Transactions on*, vol. 12, pp. 948 – 953, May 1997.

[28] H. Khodr, M. Matos, and J. Pereira, "Distribution optimal power flow," in *Power Tech, 2007 IEEE Lausanne*, pp. 1441 – 1446, July 2007.

[29] R. E. Rosenthal, "GAMS – A User's Guide," 2007.

[30] B. Kim and R. Baldick, "A comparison of distributed optimal power flow algorithms," *Power Systems, IEEE Transactions on*, vol. 15, pp. 599 – 604, May 2000.

[31] A. Conejo and J. Aguado, "Multi-area coordinated decentralized dc optimal power flow," *Power Systems, IEEE Transactions on*, vol. 13, pp. 1272 – 1278, Nov. 1998.

[32] F. Milano, "A graphical and open source matlab-gams interface for electricity market models," in *9CHLIE, Marbella, Spain*, June - July 2005.

[33] M. Bjelogrlic, M. Calovic, P. Ristanovic, and B. Babic, "Application of newton's optimal power flow in voltage/reactive power control," *Power Systems, IEEE Transactions on*, vol. 5, pp. 1447 – 1454, Nov. 1990.

[34] T. Kulworawanichpong and C. Goodman, "Optimal area control of ac railway systems via pwm traction drives," *Electric Power Applications, IEE Proceedings*, vol. 152, no. 1, pp. 33–40, 2005.

[35] M. Olofsson and E. Thunberg, "Optimal commitment of frequency converter units for railway power supply," in *Railroad Conference, 1999. Proceedings of the 1999 ASME/IEEE Joint*, 1999.

[36] D. Gonzalez and F. Manzanedo, "Power losses minimization in d.c. electric railways by means of traction substations coordinated voltage control," in *Railway Traction Systems (RTS 2010), IET Conference on*, Apr. 2010.

[37] M. Olofsson, G. Andersson, and L. Söder, "Linear programming based optimal power flow using second order sensitivities," *Power Systems, IEEE Transactions on*, vol. 10, pp. 1691 – 1697, Aug. 1995.

[38] B. Mellitt, Z. Mouneimne, and C. Goodman, "Simulation study of dc transit systems with inverting substations," *Electric Power Applications, IEE Proceedings B*, vol. 131, pp. 38–50, Mar. 1984.

[39] M. Griffiths and M. Sanders, "Energy management of traction power substations on the dallas area rapid transit system," in *Railroad Conference, 1999. Proceedings of the 1999 ASME/IEEE Joint*, p. 6, Apr. 1999.

[40] T. Kjellqvist, *On Design of a Compact Primary Switched Conversion System for Electric Railway Propulsion*. PhD thesis, Royal Institute of Technology (KTH), June 2009. TRITA-EE 2009:029.

[41] M. Olofsson, *Optimal Operation of the Swedish Railway Electrical System - An Application of Optimal Power Flow*. PhD thesis, KTH, Stockholm, Sweden, 1996.

[42] L. Abrahamsson, "Railway Power Supply Models and Methods for Long-term Investment Analysis," tech. rep., Royal Institute of Technology (KTH), Stockholm, Sweden, 2008. Licentiate Thesis.

[43] A. Bülund, P. Deutschmann, and B. Lindahl, "Circuitry of overhead contact line network at swedish railway Banverket (original title in German)," *Elektrische Bahnen*, vol. 102, no. 4, pp. 184–194, 2004.

[44] M. Olofsson, "Power Flow Analysis of the Swedish Railway Electrical System," tech. rep., Royal Institute of Technology (KTH), Stockholm, Sweden, 1993. Licentiate Thesis.
[45] GAMS, "Solver descriptions," July 2011.
[46] Norwegian national railway administration (Jernbaneverket), "Simulations Report, Railway Electric Power Supply, Ofotsbanen (original title in Norwegian)," tech. rep., Norwegian national railway administration (Jernbaneverket), 2007.
[47] H. Zhang and P. Li, "Chance constrained programming for optimal power flow under uncertainty," *Power Systems, IEEE Transactions on*, vol. 26, pp. 2417 – 2424, Nov. 2011.

Lars Abrahamsson Lars Abrahamsson was born in Luleå, Sweden in 1979. He received his M.Sc. degree in Engineering Physics from the Luleå University of Technology, Luleå, Sweden in 2005. He is currently a doctoral candidate at the department of Electric Power Systems at the Royal Institute of Technology, Stockholm, Sweden.

Stefan Östlund Stefan Östlund was born in Gävle, Sweden, in 1961. He received the M.Sc. and the Ph.D. degrees from the Royal Institute of Technology (KTH), Stockholm, Sweden, in 1985 and 1992, respectively. From 1993 to 1999, he was a Senior Lecturer at the KTH. In 2000, he was appointed Professor in electric power engineering/electric railway traction. His research interest includes electrical machines, power electronics, electric railway traction, hybrid electric vehicles and engineering education. He has been in charge of the EE curriculum at KTH since 1999 and is presently acting as Vice Dean at the School of Electrical Engineering, KTH.

Lennart Söder Lennart Söder was born in Solna, Sweden in 1956. He received his M.Sc. and Ph.D. degrees in Electrical Engineering from the Royal Institute of Technology, Stockholm, Sweden in 1982 and 1988 respectively. He is since 1999 a professor in Electric Power Systems at the Royal Institute of Technology. He also works with projects concerning deregulated electricity markets, distribution systems, power system restoration, risk analysis and integration of solar and wind power.